



Atomic-scale study of calcite nucleation in calcium oxide

Rémy Besson, Loïc Favergeon

► To cite this version:

Rémy Besson, Loïc Favergeon. Atomic-scale study of calcite nucleation in calcium oxide. *Journal of Physical Chemistry C*, 2013, 117 (17), pp.8813-8821. 10.1021/jp4002252 . hal-00833817

HAL Id: hal-00833817

<https://hal.science/hal-00833817>

Submitted on 6 Sep 2013

HAL is a multi-disciplinary open access archive for the deposit and dissemination of scientific research documents, whether they are published or not. The documents may come from teaching and research institutions in France or abroad, or from public or private research centers.

L'archive ouverte pluridisciplinaire **HAL**, est destinée au dépôt et à la diffusion de documents scientifiques de niveau recherche, publiés ou non, émanant des établissements d'enseignement et de recherche français ou étrangers, des laboratoires publics ou privés.

Atomic-Scale Study of Calcite Nucleation in Calcium Oxide

Rémy Besson*

Groupe de Métallurgie Physique et Génie des Matériaux, Unité Matériaux et Transformations,

CNRS UMR 8207, Université de Lille 1, F-59655 Villeneuve d'Ascq

Loïc Favergeon

Ecole Nationale Supérieure des Mines, SPIN-EMSE, CNRS:UMR 5307, LGF, F-42023

Saint-Etienne

ABSTRACT

In spite of its wide use, the properties of the CaO/CaCO₃ system are still far from being understood, especially the mechanisms underlying the transition between both phases. In order to investigate this issue, important in practice for storage devices, we employ first-principles atomic-scale simulations of the solid-gas interactions between CO₂ and CaO, by considering insertion of CO₂ within the subsurface, in configurations characteristic of calcite surface nucleation. Comparing the (001) and (111) surfaces demonstrates that nucleation should be strongly surface-selective, with a sharp preference for (111), and an important role of the CO₂ arrangement in the surface layer. To interpret these results, especially the important structural instabilities detected, we investigate the elastic properties of coherent CaO/CaCO₃ layered systems. This reveals the special role played by the (111) interface orientation, and confirms the behaviour detected at the atomic scale. From our study, we propose a mechanism for calcite nucleation, as well as a plausible explanation for the degradation of performances crippling the CaO-based devices used for CO₂ storage.

KEYWORDS

simulations, surface selectivity, elastic properties, CO₂ storage

INTRODUCTION

From a general point of view, the nucleation process remains misunderstood in the case of solid-gas reactions. Indeed quantitative data about the kinetics of this process are uncommon in the literature, the majority of studies remaining qualitative and dedicated to the field of thermal decomposition of solids. For example, the influence of atmosphere¹⁻⁶ and of reactant crystallography^{7,8} on the nuclei shape has been put in evidence in the case of the dehydration of copper sulfate pentahydrate. Some authors have also shown that nucleation occurs selectively at the edge of single crystals for the thermal dehydration of magnesium oxalate dihydrate⁹ and zinc acetate dihydrate¹⁰.

In this context, the CaO-CaCO₃ system appears as a good candidate in order to get better insight into these issues. Calcium oxide (CaO) and calcite (CaCO₃), connected through the reaction $\text{CaO} + \text{CO}_2 \leftrightarrow \text{CaCO}_3$ and already well-known for many practical applications, nowadays provide the framework of

important researches related with the current issue of CO₂ storage. However, in spite of recent works on CaO, devoted either to CO₂ adsorption^{11,12} or to carbonation kinetics^{13,14}, no studies have been performed so far, in order to elucidate the nucleation mechanism of CaCO₃ in CaO. This surprising deficiency may be explained by the complex crystallography of the phase transition, which raises several open issues, related in particular to the behavior of the emerging CO₃ groups, since the latter have to follow intricate paths, including reorientations, within and outside the (111) planes of the oxide. As a consequence, it is difficult to propose, from phenomenological considerations, a mechanism for the formation of a calcite nucleus. These difficulties justify resorting to theoretical investigations, which forms the subject of the present paper.

In a solid-gas system, the nucleation of a new phase occurs in general at or near surfaces, the latter usually displaying a local enrichment in gaseous species, providing configurations that can be viewed as precursors for nuclei. In the case of CaO, however, a previous study of the (001) surface¹⁵ pointed out that, in experimental conditions favourable to calcite nucleation, the coverage of this surface by CO₂ should be much lower than a full layer. This previous study supports the possibility that CaO carbonation may occur through a localized mechanism, by emergence of nanometric isolated nuclei. Such a localized aspect of nucleation has been observed in the case of decomposition reactions such as Li₂SO₄·H₂O dehydration¹⁶ or KAl(SO₄)₂·12H₂O dehydration¹⁷, where small domains of the new solid phase were observed at the surface of the initial one. Although surface defects (point defects, steps,...) are usually regarded as important for the nucleation of a new phase¹⁸, it is logical in any first-principles study to begin by considering perfect surface zones. This model framework will demonstrate its efficiency, since our study will evidence clear-cut trends and provide a sound background for future steps, possibly including initial surface defects and quantifying their influence on the nucleation process.

The purpose of the present paper will be to explore this hypothesis, by making use of ab initio atomic-scale methods. Because this surface was predicted as being of lowest energy¹⁵, the (001) surface will be considered first. Moreover, since the (111) planes of CaO are expected to play a special role in calcite nucleation, in relation with the morphology of calcite, the (111) surface will be studied next, in similar conditions. In both cases, our analysis will be inspired from the classical nucleation theory (CNT), which primarily provides nucleation curves through an estimation of bulk, interface and elastic contributions to the energy of a nucleus. In the case of CaO/CaCO₃, however, the low symmetry will not allow to evaluate separately the last two contributions. We will thus prefer an “integrated” simulation approach previously applied fruitfully to Al-Cu alloys¹⁹, which gives, in principle, direct access to nucleation curves, without resorting to any artificial, and probably unrealistic, bulk/interface/elastic decomposition.

Our atomic-scale investigations will demonstrate clear-cut trends as regards the interactions between CO₂ and CaO surfaces, allowing to draw conclusions on CaCO₃ nucleation. In order to help interpreting these nanoscale results, it will be useful to remark that the CaO → CaCO₃ transition can be viewed as a sequence of CO₂ insertions into the oxide, accompanied with a strong elastic distortion of the Ca₂O₂ rhombohedron, the free and CO₂-doped lattices remaining fully coherent. This justifies adopting, as a background for analysis, a macroscopic point of view based on elasticity criteria. To this aim, an efficient way consists in employing the so-called “constituent strain energy” (E_{cs}) approach, developed previously for metallic, first cubic²⁰ and more recently hexagonal²¹, alloys, and which allows to identify elastically soft directions, corresponding to favourable lattice planes for

incipient nuclei. For CaO/CaCO₃, we will make use of an original flavour of the E_{cs} analysis, including several major new features, due in particular to the requirement to take into account anharmonic effects. Whereas this is a common hypothesis for metallic systems, neglecting these effects is not realistic in oxides and other minerals. The application of the E_{cs} methodology to CaO/CaCO₃ will prove to be fruitful, confirming, and shedding new light on, the atomic-scale results.

METHODS

In this work, the ab initio calculations were performed using the Vasp software^{22,23}, implementing the Density Functional Theory with plane waves and pseudopotentials within the Projector Augmented Wave method. The GGA exchange-correlation was employed, with the Perdew-Burke-Ernzerhof functional²⁴. The cutoff energy for plane waves and k-mesh in reciprocal space were chosen equal to 600 eV and 4x4x4 (for a single Ca₄O₄ cubic unit cell), these values leading to sufficient convergence (< 1meV/atom) for all results. The (001) surface was studied with a supercell containing 2x2x4 Ca₄O₄ cubic unit cells (128 atoms), this size being previously found¹⁵ to be sufficient to prevent spurious interactions between both surfaces in periodic conditions. Because this corresponds to realistic conditions for surfaces, the size of the system within the interface plane was held fixed in all simulations, while its thickness, perpendicular to the interface, was allowed to relax, as well as all atomic positions. The (111) surface was studied in similar conditions, using a supercell with 2x2x2 Ca₁₂O₁₂ unit cells (192 atoms).

The present work relies on the atomic-scale full evaluation of the energy change associated with the creation of a calcite nucleus, defined by the number of CO₂ molecules inserted into CaO to build this nucleus. This approach, labeled below as “direct study of nucleation”, contrasts with numerous more usual works on this topic using the classical threefold – bulk+interface+elastic – decomposition of the total energy associated with a nucleus. Inspection of the literature indicates that the few previous direct studies of nucleation¹⁹, performed by means of empirical (EAM) interatomic potentials designed for Al-Cu metallic alloys, made use of a simplified scheme, by imposing a constant global composition in the whole [matrix+nucleus] system, which offers the practical advantage of dispensing from detailed evaluation of the chemical potentials in the matrix, at the expense however of imposing an artificial, possibly unrealistic, composition profile around the nucleus, depending on the size of the latter. In the present case of CaO//CaCO₃ by ab initio methods, such a procedure is clearly untractable, due to the much more limited size of the whole system accessible from ab initio calculations. Nevertheless, this is not a critical issue for our purpose, since the energy change associated to nucleus formation can be written generally as:

$$\Delta E(N_{CaO}, N_{CO_2}) = E_{SC}(N_{CaO}, N_{CO_2}) - N_{CaO} E_{CaO}^{ref} - N_{CO_2} \mu_{CO_2} \quad (1)$$

where E_{sc} is the total ab initio energy for a system (supercell) nucleus containing a given number of CO₂ molecules. Since we are not interested here in effects related to CaO off-stoichiometry, an issue left for future work, it will be consistent to use throughout the energy E_{CaO}^{ref} of perfect bulk CaO (for a unit cell). Moreover, the oxide being at equilibrium with the CO₂ gas phase, the chemical potential of CO₂ will have to be introduced. In this work, μ_{CO_2} is assimilated to the energy of an isolated CO₂ molecule, calculated with the same ab initio method, namely $\mu_{CO_2}^0 = -22.943$ eV. This amounts to keep only the T = 0 K energy contributions, assuming that vibration parts cancel out in relation (1). At the same level of approximation, i.e. neglecting vibrations and off-stoichiometry in the bulk CaO

and CaCO_3 solid phases, the equilibrium condition (CaO stable for $\mu_{\text{CO}_2} < \mu_{\text{CO}_2}^{\text{equ}}$) reads $\mu_{\text{CO}_2}^{\text{equ}} \approx E_{\text{CaCO}_3}^{\text{ref}} - E_{\text{CaO}}^{\text{ref}} = -24.720 \text{ eV}$. This demonstrates that the $\mu_{\text{CO}_2}^0$ value chosen above consistently lies within the stability domain of calcite, as required for the study of CaCO_3 nucleation. Indeed, regarding CO_2 as a perfect gas, which is an adequate approximation in the (T,P) domain relevant for nucleation, μ_{CO_2} is a strongly decreasing (resp. weakly increasing) function of T (resp. P), and $\mu_{\text{CO}_2}^0$ therefore provides an upper bound of μ_{CO_2} , hence conditions extremely favourable to CaCO_3 formation. Therefore, the present analysis could probably be refined by taking into account more accurately the influence of μ_{CO_2} , but this is left for future works.

As mentioned briefly above, the crystallography of the cubic $\text{CaO} \rightarrow$ trigonal CaCO_3 transition (Fig. 1) is usefully described as a pair of $\text{CO}_2 + \text{CaO} \rightarrow \text{CO}_3$ substitutions, within the (111) planes of cubic CaO , switching from the initial Ca_2O_2 rhombohedron to a larger $\text{Ca}_2\text{C}_2\text{O}_6$ rhombohedron, with a change of lattice parameters from (33°, 5.88 Å) to (46°, 6.37 Å). For volume reasons, the CO_3 groups in adjacent (111) planes have opposite orientations, giving rise to two kinds of groups, G1 and G2, deduced from each other by a 180° shift. Moreover, a second type of rotation within (111) should be considered. More precisely, the interstitial sites in the NaCl structure of CaO , at positions of type (1/4,1/4,1/4), are located along the $\langle 111 \rangle$ atomic rows. Considering that additional oxygen should occupy these sites provides naturally a reference mode for CO_2 insertion, thus noted “i0°” below (0° meaning “no rotation”). However inspection of the CaCO_3 unit cell indicates that the CO_3 groups in this structure display an orientation shifted by 30°, hence noted “i30°”, the same G1/G2 distinction applying as well to CO_3 groups in i0° or in i30° modes. The (001) (respectively (111)) surface is made of a stacking of mixed [Ca+O] (resp. pure Ca or O) layers, and the n^{th} layer below the surface will be referred to as “Ln” throughout, L0 and L1 being thus the surface and subsurface layers.

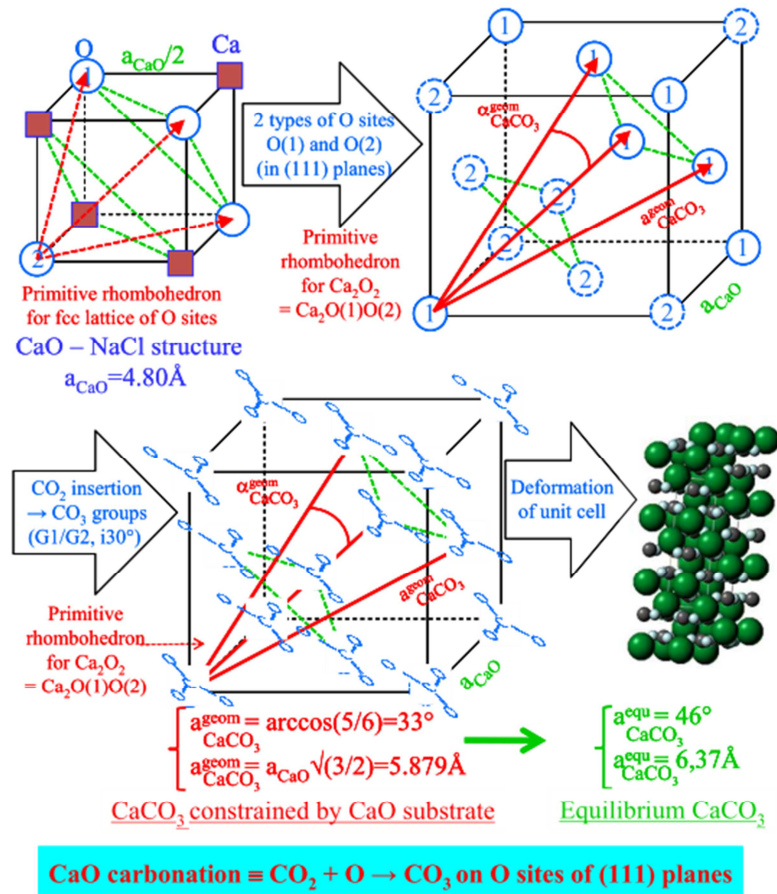


Figure 1 : Schematics of the carbonation process of calcium oxide, with $\text{CO}_2 + \text{O} \rightarrow \text{CO}_3$ substitutions leading to calcite.

RESULTS

As mentioned previously, our purpose consists in investigating the possibility of calcite nucleation, through a sequential mechanism involving successive aggregations of CO_2 up to the size of the critical nucleus. According to the remarks of the previous section, several cases are to be considered, corresponding to $i0^\circ/i30^\circ$ modes, G1/G2 groups, as well as L0, L1,... surface layers. Leaving the kinetic aspects for future work, we consider here the net products of the transitions, namely the stabilities and energy costs of various kinds of CO_2 insertion.

(001) Surface. The results of single CO_2 insertion for the $i0^\circ$ mode within the L0 layer are displayed on Figure 2(a,b), for G1 and G2 orientations of the CO_3 groups. Surprisingly, both configurations are found to be unstable, G1 leading to full CO_3 rejection above the surface, while G2 returns to a configuration typical of CO_2 adsorption. Similar instabilities (not displayed for brevity) are also found with the $i30^\circ$ mode, leading to an adsorbed state similar to that of Fig. 2b. As CO_2 penetration into the surface must entail strong local elastic strains, hence possibly significant interactions between the CO_2 molecule and its periodic images, it is important to check that the limited size ($2 \times 2 \times 4$ unit cells) of the supercell is not critical in these conditions, namely that CO_2 rejection is not due to spurious repulsive interactions between inserted molecules. To carry out this verification, a similar calculation was performed for CO_2 in L0 layer, with a more extended $3 \times 3 \times 4$ supercell (288 atoms) allowing a larger separation between CO_2 molecules, and this test led to the same final state,

confirming the conclusion of instability of CO₂ in the (001) surface. Therefore, insertion of CO₂ into the surface layer can thus not be considered as a realistic initial stage for nucleation in the (001) surface. However, the situation is significantly different for insertion into the subsurface (L1) layer, as illustrated on Figure 2(c,d): all i0°/i30° and G1/G2 configurations lead to stable insertion states, characteristic of CO₂ behaviour in the (001) subsurface. It should be noted that, whereas the i30° mode, typical of calcite structure, is found to be stable in bulk CaO, this mode is destabilized by the (001) surface, which systematically entails a i30° → i0° reorientation of initially i30° configurations. At this stage of the analysis, L1 insertion thus appears as a possible initial step for nucleation.

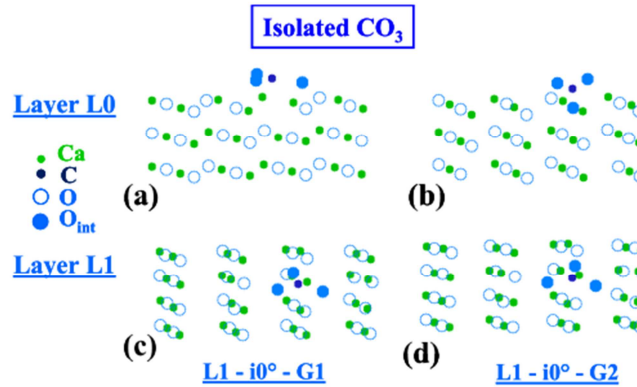


Figure 2 : Equilibrium configurations after insertion of isolated CO₂ inside the (001) surface of CaO: in the surface (L0) layer (top pictures), in the subsurface (L1) layer (bottom pictures).

The previous hypothesis of initiation of the nucleation process by a single CO₂ molecule being crippled by strong instabilities, an alternative may be provided by the possibility of collective stabilization of CO₂ inserted clusters. This scenario may seem reasonable, in consideration of the structure of calcite, made of layers of CO₃ groups in i30° mode, with alternating G1/G2 orientations in two neighbouring (111) planes. More precisely, the stability of bulk calcite is due to attractive interactions between CO₃, possibly of two types (i) G1-G1 or G2-G2 within a single (111) plane and (ii) G1-G2 between two adjacent (111) planes, and these interactions may also be responsible for the stabilization of a nanoscale nucleus. To investigate this issue, it is useful to consider CO₂ doublets, the first question being as to whether a collective effect may stabilize the previously found unstable L0 configurations. Careful inspection of the various possibilities, with either intra- or inter-(111) plane relative CO₂ positions, reveals that the answer is definitely negative: the presence of a second CO₂, either in L0 or in L1, does not prevent rejection of the L0 molecule, whatever the orientation G1-G1, G2-G2 (intra-(111)) or G1-G2 (inter-(111)) of the CO₂ doublet, and for both the i0° and i30° modes. Conversely, restricting to subsurface (L1) doublets confirms the favourable trend noted previously for isolated CO₂, although with a net distinction between intra- and inter-(111) configurations (respectively Fig. 3a and 3b). As evidenced on the figures, the former ones correspond to important reorientations of the CO₃ groups out of the (111) planes, while the latter lead to much more reduced local perturbations. In spite of these qualitatively distinct behaviours, the energy dispersion is moderate (< 1.5 eV) between the various configurations. Here again, the i30° mode systematically converts to i0°, which suggests that the emergence of groups of CO₃ in i30° mode, characterizing calcite, is delayed until the nucleus has become larger.

The previous analysis has pointed out that the subsurface should be a privileged zone for calcite nucleation below the (001) surface. It was however limited to CO_3 doublets, and the next step consists in increasing the nucleus size. However, this is a hardly achievable task, due to the limited supercell size consistent with ab initio calculations, as well as the high configuration entropy associated with larger CO_2 clusters. For the same reasons, exploring the process of lateral extension of the nucleus within the L1 layer would be interesting, but beyond the scope of current ab initio methods. We thus considered more compact configurations involving four and six groups of CO_3 . In all cases, the requirement of compactness implies intra, as well as inter-(111), configurations, hence significant reorientations out of the (111) planes, giving the relaxed state an irregular aspect not expected from a CaCO_3 nucleus. Figure 3(c,d) illustrates this result in the case of a nucleus containing six CO_3 groups.

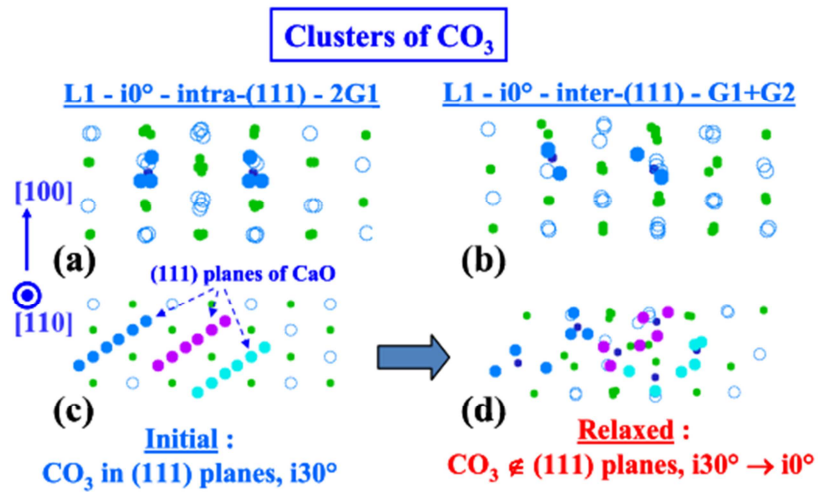


Figure 3 : Insertion of CO_2 clusters into the (001) surface: (a) and (b) doublets with interactions intra- and inter-(111) planes, and compact 6- CO_2 cluster (c) initially and (d) at equilibrium.

In spite of these difficulties attached to the identification of a realistic calcite nucleus in the (001) surface, it is instructive to gather the above results in an attempt to build a “nucleation curve” for this surface. Figure 4 displays the result, and the most striking feature is the oscillating, rapidly saturating profile, without monotonic trend when increasing the cluster size. It should be noted that figure 4, which corresponds to equation (1), only reflects the nucleation curve to within an offset depending on the initial adsorption level of the zone in which the nucleus appears. To precise this point, the figure displays the energy levels $E_{\text{ads}}(\omega)$ typical of various degrees ω of adsorption. Therefore, assuming that nucleation occurs in a zone initially with an adsorption level ω_0 , the “net” energy profile for nucleation is $E_{\text{nucl}} = \Delta E - E_{\text{ads}}(\omega_0)$. This provides a basis to compare the different situations that may occur a priori for nucleation, namely (1) in a zone of unadsorbed (“fresh”) surface or (2) in a zone with initially adsorbed CO_2 clusters. Case 2 may itself be divided into two subcases, depending on whether CO_2 insertion leads to an expulsion of the adsorbed molecules (case 2a), or preserves them (case 2b). The latter possibility is probably the most intricate one, as should involve interactions between adsorbed and inserted molecules. Keeping in mind these pictures, Figure 4 indicates that case 1 should prevail, namely that nucleation in a zone of quasi “fresh” surface should be more favourable (i.e. with a lower energy barrier) than in a more heavily preadsorbed area. Whereas this conclusion relies on the comparison between “fresh” and “adsorbed” energy levels, the latter being deeper, it may be brought qualification related to the extremal value

chosen for the CO_2 chemical potential, as explained above. Reducing this parameter, hence the intensity of the supersaturation, would result in further promoting the fresh areas with respect to their adsorbed counterparts, thus lowering the energy barrier associated with nucleation in preadsorbed zones, and favouring situation 2. In this case, the various unstable CO_2 doublets, as already described, readily provide configurations mixing CO_2 adsorption and insertion in the same surface portion, namely under the assumption that adsorption is locally maintained, rather than swept out, by insertion (case 2b). Although detailed investigation of this scenario is complex and lies beyond the scope of this work, it is instructive to consider one such instance, as displayed on figure 4 for $n=1$ and $\omega = 1/8$, which suggests that the interaction between the incipient nucleus and the adsorbed molecules may not be critical, and possibly favourable, for nucleation. On the whole, our analysis does not rule out, from energy criteria, the possibility of calcite nucleation within a (001) surface. However, this does not appear as a favourable process, due to the strong structural perturbations induced by CO_2 insertion, especially the reorientations of the CO_3 groups out of the (111) planes, which drastically decay the similarity with a realistic CaCO_3 nucleus.

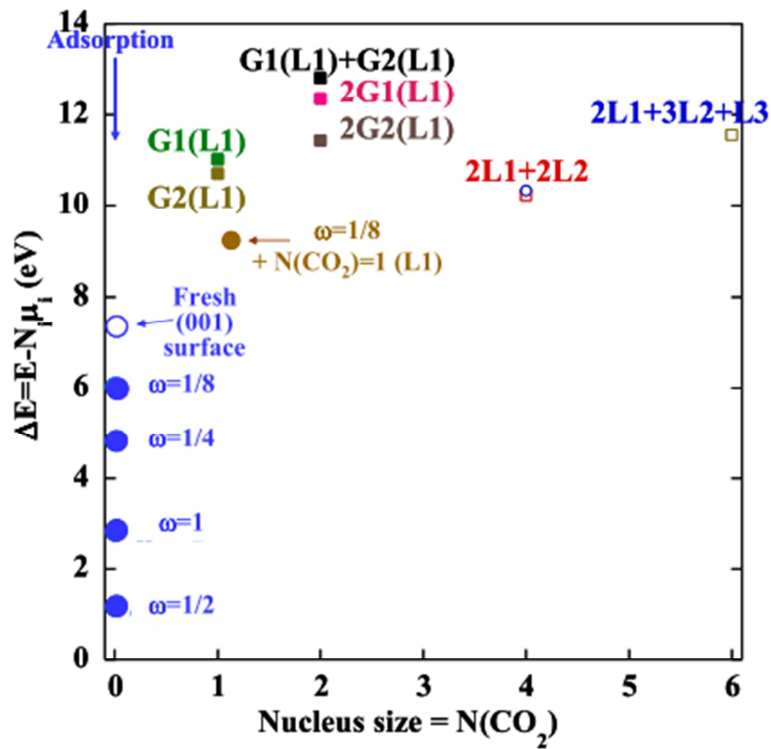


Figure 4 : Adsorption-insertion energetics for CO_2 in the (001) surface of CaO ; ω refers to various levels of adsorption.

(111) surface. The layered structure of calcite, inducing a particular role of the (111) planes, makes it particularly relevant to perform a similar study on the (111) surface of CaO . To help understanding this point, Figure 5 displays the effect of a sequence of two substitutions $\text{O} \rightarrow \text{CO}_3$, using $i30^\circ$ mode, initially in calcium oxide (figure 5a), leading successively to Ca_2CO_4 (figure 5b) and $\text{Ca}_2\text{C}_2\text{O}_6$ (figure 5c). Comparison of figure 5c with real calcite (figure 5d) clearly shows the similarity between the two structures, except the large difference in rhombohedral angles and lattice parameters due to the expansion within (111) planes induced by the CO_3 groups.

Sequence of two $O \rightarrow CO_3$ ($i30^\circ$) substitutions in (111) planes of Ca_2O_2

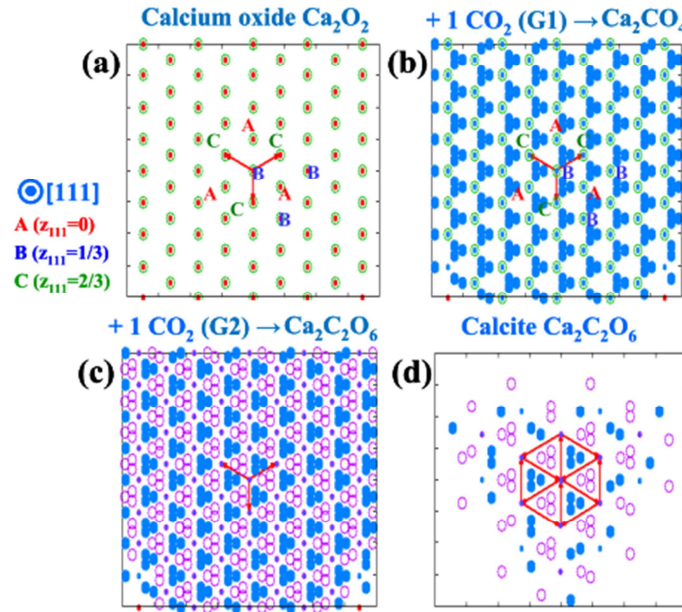


Figure 5 : Detail of the sequence of two substitutions $O \rightarrow CO_3$ ($i30^\circ$) in Ca_2O_2 leading to the calcite structure (view along $[111]$ direction of the oxide) : (a) oxide unit cell, (b) first CO_2 insertion (G1), (c) second CO_2 insertion (G2), (d) equilibrium calcite structure, showing similarity with (c).

This analogy suggests that the mechanism of calcite formation might involve (111) layers of CO_3 , and we now explore this possibility by investigating insertion of CO_2 in the (111) surface. Fig. 6 to Fig. 8 display the relaxed structures resulting from $O \rightarrow CO_3$ insertions of increasing amounts of CO_2 molecules into the surface (L0) layer. For the simplest case of isolated CO_3 (Fig. 6), the insertion is found to be stable within the (111) plane, which contrasts with the persistent instabilities detected in the (001) surface. Moreover, as already noted for the (001) surface, the $i30^\circ$ mode is found to switch to $i0^\circ$, which confirms that further investigations, beyond the scope of this work, would be useful to determine the conditions leading to the $i0^\circ \rightarrow i30^\circ$ transition typical of calcite formation.

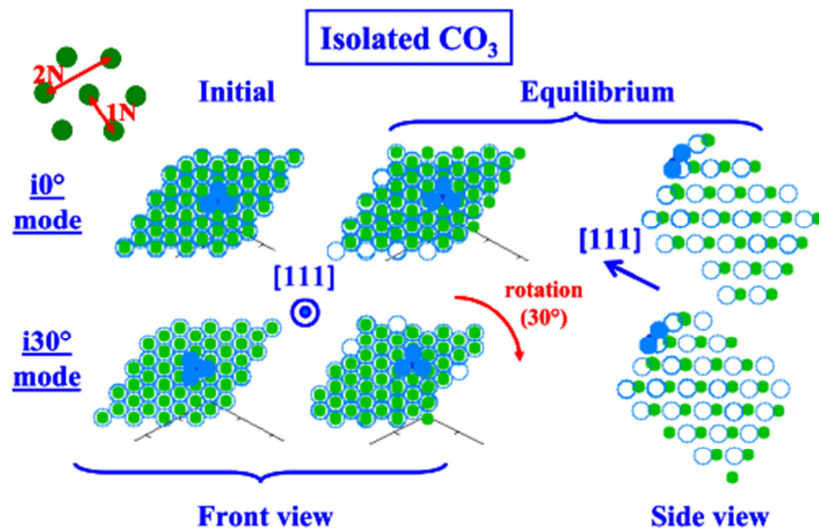


Figure 6 : Insertion of isolated CO_3 within the (111) surface of CaO (L0 layer): initial configurations (left) and relaxed ones (middle and right).

Increasing the number of CO_3 groups in order to sketch an incipient nucleus of calcite, it is convenient to introduce the level of neighbourhood of these groups, distinguishing here first- (1N) and second-neighbour (2N). A doublet of CO_3 in 1N configuration (Fig. 7) is found to be unstable, decaying towards adsorption. Indeed, this trend is less definite than for the (001) surface, since insertion may possibly be stabilized by tuning the C-O distance initially specified in the simulation. However, thermal movements should preferentially lead to instabilities. Figure 7 also displays the case of a 1N triplet: surprisingly, possibly due to the order 3 symmetry, this configuration is found to be stable in insertion, though significant tilt of the groups occurs out of the (111) planes. Comparing the initial and relaxed states indicates that the CO_3 groups repel each other, being no longer centered on the O sites. Moreover, each group creates two O-O doublets with O ions from neighbouring sites, leading to local atomic arrangements very different from calcite. On the whole, it is therefore unlikely that 1N configurations play a role in calcite nucleation (we will return on this point below).

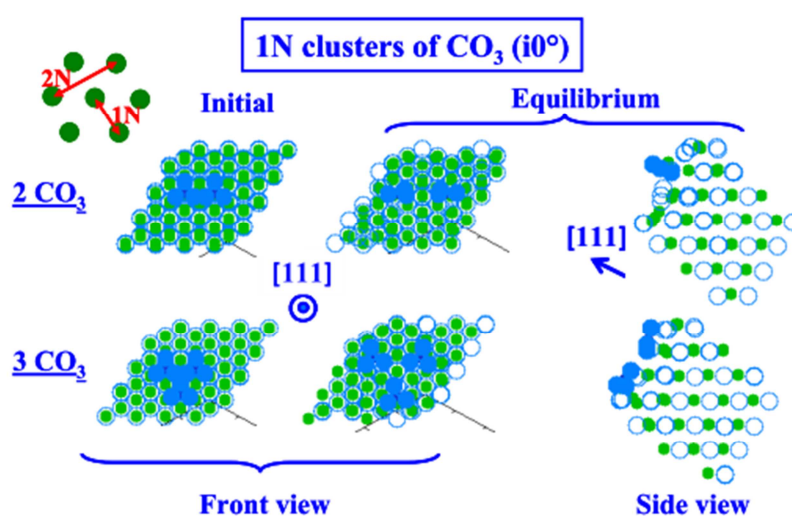


Figure 7 : Insertion of 1N clusters of CO_3 within the (111) surface of CaO (L0 layer): initial configurations (left) and relaxed ones (middle and right).

The situation is totally different for the 2N doublet (Fig. 8a), which is found to be stable and to induce very limited local perturbations, which makes it a serious candidate in elucidating the nucleation process. As will be precised below from energy criteria, 2N CO_3 are almost energetically independent, which is reflected by the $i30^\circ \rightarrow i0^\circ$ decay which persists when going from the isolated CO_3 to the 2N doublet. Increasing the number of 2N groups raises strongly the configuration entropy, and selected configurations with four groups are displayed on Fig. 8b. This confirms that 2N arrangements are favourable, corresponding to a maximum theoretical rate of insertion coverage equal to 1/3. Reminding the 1N instability, configuration 2 with four CO_3 is interesting, since it involves interactions with 1N groups in the image supercells, which however do not lead to instabilities, rather to distortions bringing the CO_3 groups somewhat closer to the $i30^\circ$ mode. This might be a hint of the existence of scarce 1N arrangements as isolated “faults” within an otherwise globally 2N surface repartition of CO_3 (in $i0^\circ$ mode), these faults being possibly related with the $i0^\circ \rightarrow i30^\circ$ reorientation characteristic of CaCO_3 . This hypothesis would require further investigations, which are however hardly tractable by ab initio methods due to the larger scale involved. Moreover, while the present work is limited to the outer (L0) layer of the (111) surface, investigations of the properties related with in-depth growth of the nucleus (L1 layer and beyond) would provide a

more comprehensive picture of calcite nucleation. This however requires a realistic description of the CO_2 arrangement in the L0 layer, which cannot be reached from the limited supercells handled in ab initio calculations. Empirical force fields would thus be very useful for such purposes.

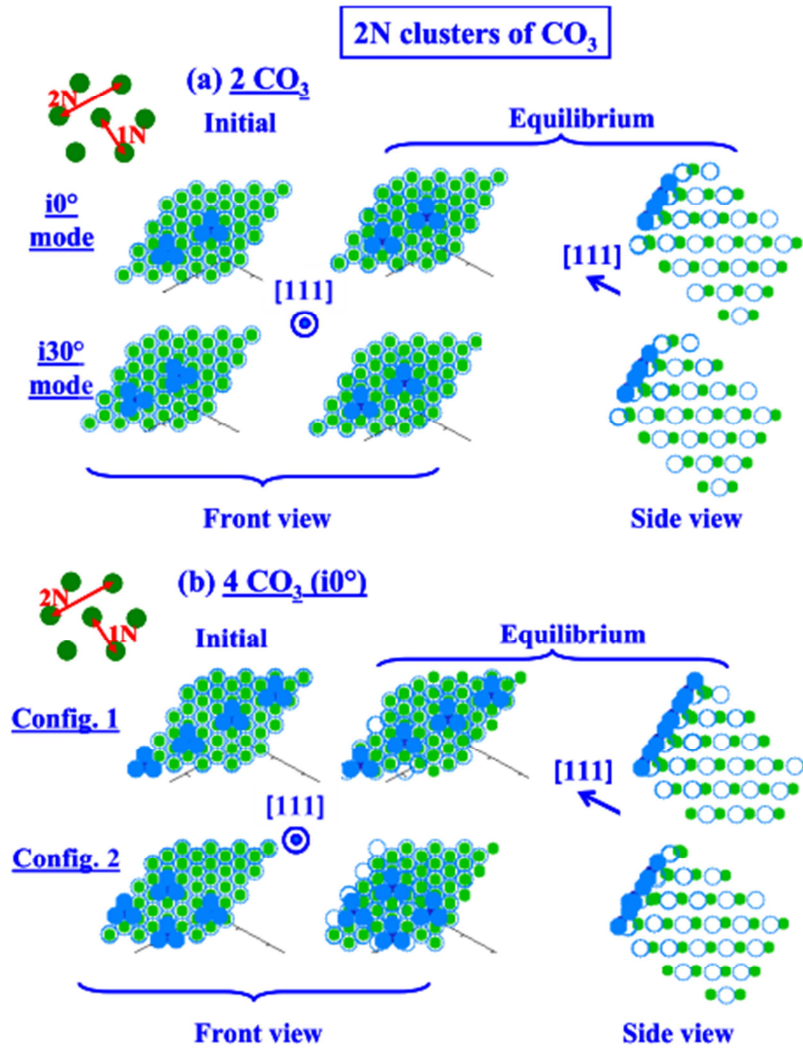


Figure 8 : Insertion of $2N$ clusters of CO_3 within the (111) surface of CaO (L0 layer): initial configurations (left) and relaxed ones (middle and right).

Following the same lines as for (001) , these results can be gathered to delineate a nucleation energy profile for the (111) surface, including various configurations of insertion and adsorption (Figure 9). It should be noted that the order of magnitude of ΔE , much higher than for the (001) surface, is due to the presence, in the supercell, of a couple of surfaces with different termination planes, namely, besides the surface with O termination, relevant for our study, a second one with Ca termination. However, since we are concerned merely with energy differences between incipient nuclei and fresh/adsorbed zones, this feature is immaterial for our study. Here again, the adsorption states are found more favourable than the fresh surface, which suggests that CO_2 adsorption on CaO is rather surface-insensitive. Conversely, the most striking result is related to the behaviour of $2N$ configurations with increasing numbers of inserted CO_3 . The energy follows a quasi linear profile, reflecting the mutual independence of $2N$ CO_3 up to maximum insertion coverage of $1/3$. The slope is determined by the CO_2 chemical potential, and inspection indicates that the critical value for this

parameter, corresponding to a switch from positive to negative slope, is $\mu_{CO_2}^{ins} = -23.748 eV$ (negative slope for $\mu_{CO_2} > \mu_{CO_2}^{ins}$, as in Figure 9). Since $\mu_{CO_2}^{ins}$ lies in the stability domain of calcite, i.e., $\mu_{CO_2}^{eq} < \mu_{CO_2}^{ins} (< \mu_{CO_2}^0)$, there should exist a critical supersaturation to be reached in order to initiate the arrangement of 2N CO₃ groups. This is consistent with viewing this arrangement as a precursor of calcite, which should therefore nucleate first by extending laterally within the L0 layer, before starting in-depth growth. Comparison with the previous study of the (001) surface leads to conclude that calcite nucleation should be strongly surface-selective, (111) representing probably a very favourable surface. Moreover, the maximum 1/3 coverage is much lower than required for calcite. As a consequence, this compound should form primarily in a strongly defected state, implying a large density of CO₂ vacancies. As already pointed out, atomic-scale investigations of larger CO₃ arrangements remain, for the time being, beyond the scope of ab initio methods. The previous remark, about the effect of μ_{CO_2} on the adsorption vs fresh levels, also holds for the (111) surface, but the energy dispersion of configurations locally mixing adsorption and insertion (situation 2b) confirms that this issue would require a more detailed analysis.

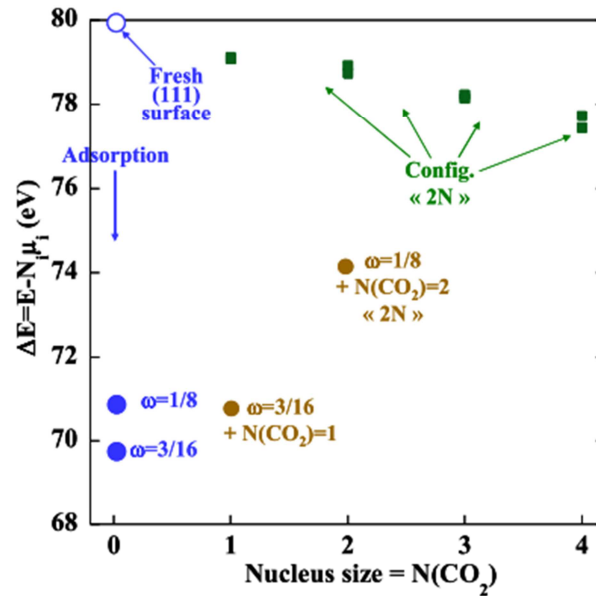


Figure 9 : Adsorption-insertion energetics for CO₂ in the (111) surface of CaO ; ω refers to various levels of adsorption.

Taking into account the previous results, a layer-by-layer mechanism for calcite formation on the (111) surface of CaO may thus be sketched as follows:

- 1) Nucleation of a surface (L0) arrangement of CO₃ groups of 2N type (maximum coverage 1/3);
- 2) In-depth growth by formation of similar arrangements in deeper (L1,L2,...) layers: the required diffusion of CO₂ across the existing layers is made easier by a large proportion of vacancies;
- 3) i0° → i30° transition for a sufficient thickness, probably related with critical lattice parameters between those of CaO and CaCO₃.

This mechanism requires no loss of coherency, rather a progressive shift towards CaCO_3 . It should be noted that this scenario of lateral nucleation and layer-by-layer growth of CaCO_3 , is consistent with other results from calculations (not shown for brevity) of CO_2 doublets inserted in adjacent layers, showing that such a hypothesis, related to in-depth nucleation, is less favourable. In spite of the surface selectivity of nucleation, comparing Figs. 4 and 9 interestingly suggests that the (001) and (111) surfaces are close with respect to the energy barriers for insertion from a fresh/adsorbed surface. This similarity contrasts with the structural features of CO_2 insertion, which are markedly surface-dependent: whereas the formation of CO_3 groups in the (111) surface (excepting 1N cases) appears to be an easy process, its (001) counterpart entails strong structural changes, in particular reorientations.

DISCUSSION

Our atomic-scale study has pointed out CO_2 vacancies in calcite as essential in the nucleation process, at least in its very early stages. The question thus arises as to whether the favourable role of these defects can be inferred from alternative approaches, especially CNT analysis. More precisely, a recent work on the nucleation of zirconium hydrides²⁵, combining atomic-scale simulations and CNT, has demonstrated that the chemical driving force for nucleation may be drastically increased by off-stoichiometry within the nucleus. In order to determine if a similar effect may be expected in the $\text{CaO} \rightarrow \text{CaCO}_3$ transition, we found it convenient, using ab initio calculations, to investigate the influence of increasing amounts of CO_2 on the energetics of CaO , added in doublets (G1+G2) for consistency with the calcite structure (see Figs. 1 and 5). Figure 10 displays the results for $2 \times 2 \times 2$ unit cells of Ca_2O_2 , showing a surprisingly linear behaviour, the energy being consistent with that of CaCO_3 when the number of doublets increases. This indicates the limited interactions between these doublets, in contrast with a previous study of CO_2 adsorption on the (100) surface of calcite¹⁵, which pointed out that the lateral interactions between adsorbed molecules cannot be neglected.

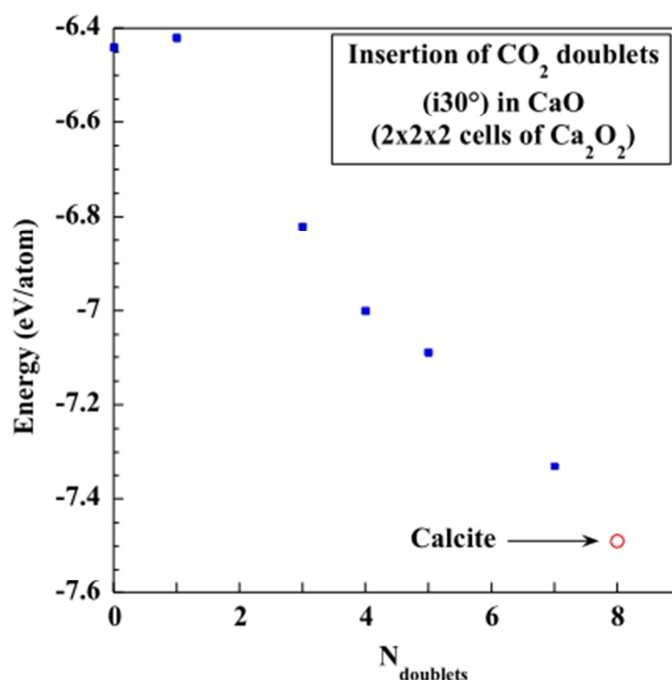


Figure 10 : Insertion of CO_2 doublets (G1 + G2) in bulk CaO .

From the data of figure 10, the bulk driving force for nucleation can be estimated, as a function of the nucleus size ($N(\text{CO}_2)$) and off-stoichiometry (x) measured by the proportion of O_{CaO} sites not occupied by CO_2 (i.e. CO_2 vacancies in the $\text{CaCO}_3(x)$ compound). Figure 11 shows that the bulk driving force (negative if favourable for nucleation) is strongly reduced by CO_2 vacancies in calcite. This demonstrates that a chemical driving force argument promotes perfect, vacancy-free calcite, implying that CO_2 vacancies should have a transient role limited to the first stages of nucleation, and that CaCO_3 with increasing thickness should progressively recover stoichiometry, in agreement with the nucleation mechanism proposed above. In particular, as suggested by the above study of the (111) surface, these defects may be important by (i) reducing the elastic energy cost for CaCO_3 formation, and (ii) possibly allowing CO_2 diffusion within the CaCO_3 layer.

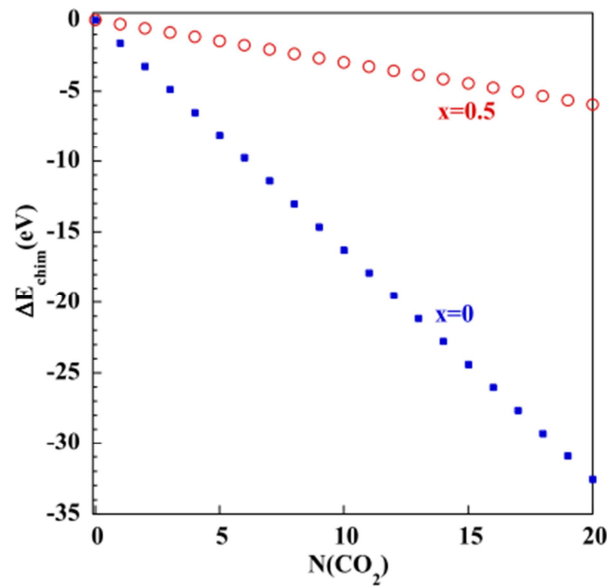


Figure 11 : Effect of calcite off-stoichiometry (x = fraction of CO_2 vacancies in the CaCO_3 structure) on the chemical driving force for nucleation.

Another important question concerns the interpretation of the strikingly different behaviours of the (001) and (111) surfaces with respect to nucleation, as inferred by the present results. As a “bulk driving force” effect, connected with surface-dependent epitaxy strains implying surface-dependent nucleus off-stoichiometry, is not relevant (figure 11), other factors should be investigated, among which the possibility of surface-dependent elastic energies. The macroscopic-scale approach relying on “constituent strain energies” (E_{cs}) may provide further insight into this issue. The background on E_{cs} has been given elsewhere^{20,21}, and the reader can refer to these previous works for details. We will merely recall here that this method allows to obtain elastic energies of long-period multilayers (here CaO/CaCO_3) with various interface planes, hence providing hints of preferential habit planes for coherent nuclei. In the long-period limit, the interface energy becomes negligible, which only leaves the elastic contribution. As developed for the present work, this approach possesses several originalities that will not be described in detail here: most importantly, we introduce a fully numerical approach, designed to yield the minimum elastic energy of the multilayer with respect to the full strain tensors of both media, these tensors being simply connected by a general, unrestricted relation of epitaxy within the interface plane. This numerical scheme allows major improvements which remained beyond the scope of previous studies, namely (i) elasticity analysis in a mixed cubic/trigonal coherent system such as CaO/CaCO_3 , (ii) arbitrary strains in both media, including all

strain components out of the interface plane, (iii) account for anharmonic elastic constants, up to third order for trigonal calcite, and to fourth order for the cubic oxide. It should be noted that E_{cs} considerations are related with bulk properties, while the present atomic-scale work was concerned with surface nucleation.

However, in spite of this discrepancy, this macroscopic approach will prove fruitful in helping to interpret the atomic-scale results. Moreover, since our fully numerical E_{cs} analysis overwhelms difficulties (points (i)-(iii)) crippling previous works, it opens new areas of investigations of elastic energies in alloys, especially as regards cubic metallic systems for which accurate high-order elastic constants are now becoming available²⁶. As regards CaO//CaCO₃, calculating E_{cs} with anharmonicity requires many elastic constants. All these quantities were taken from the literature, with measured values²⁷ for CaCO₃, and calculated ones²⁸ for CaO. In the latter case, it should be noted that the use of an empirical force field imposed Cauchy relations between these constants, and an improvement, left for future work, would consist in using ab initio methods in order to obtain all these quantities with higher accuracy. This would allow a more quantitative estimation of elastic energies in CaO//CaCO₃. Our purpose here is more limited, since we merely wish to investigate the relevance of using E_{cs} as a criterion to understand, in terms of elastic energies, the striking difference between the (001) and (111) surfaces. To this aim, we performed E_{cs} calculations for CaO//CaCO₃ with equal amounts of both phases ($x(\text{CaO}) = 0.5$), either neglecting (figure 12a) or including (figure 12b) anharmonicity. Without anharmonicity, the E_{cs} shape appears rather isotropic, with no privileged direction, and the order of magnitude is very high, reflecting the large lattice misfit between both phases. Conversely, introducing anharmonicity leads to a significantly different behaviour, since no numerical solution can be reached around the [111] direction, namely around the (111) interface plane. Detailed investigation indicates that such instabilities are probably due to the selected values of third and fourth order elastic constants of CaO, which confirms that more accurate assessments would be helpful. Nevertheless, comparison between Figs. 12a and 12b suggests that anharmonic effects are mostly felt around [111], a possible cause for strong lowering of the elastic energy around this direction. This conclusion is encouraging, since it precisely corresponds to CaCO₃ layers located within (111) planes. It provides a further argument in favour of highly anisotropic calcite nucleation, this phenomenon being limited to the (111) surface. Moreover, we already mentioned that the (001) and (111) surfaces mainly differ for structural features related with CO₂ insertion (reorientations, instabilities,...), whereas the global energy levels are rather similar in both surfaces. Comparison with Figs. 12a and 12b reveals that overall surface-independent energetics is reasonably captured by harmonic elasticity, while anharmonicity monitors the structural, surface-dependent, discrepancies. Further insight into this point can be gained by considering CaO//CaCO₃ for $x(\text{CaO}) = 99\%$ (figure 12c), namely if the behaviour only depends on the elastic constants of the thin CaCO₃ layer (the constants of CaO having no effect). The shape of E_{cs} being close to that of Fig. 12a, the structural surface-dependent effects should be related to the anharmonicity of CaO rather than CaCO₃.

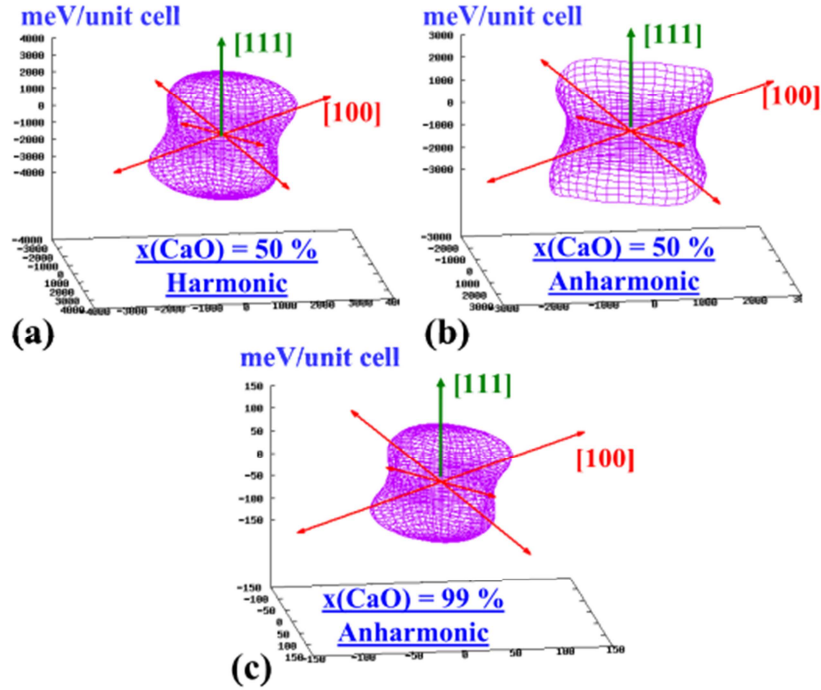


Figure 12 : Constituent strain energies of CaO//CaCO₃ layered systems, (a) $x(\text{CaO}) = 50\%$ in the harmonic approximation, (b) $x(\text{CaO}) = 50\%$ including anharmonic effects, (c) $x(\text{CaO}) = 99\%$ including anharmonic effects (see text for details). For each crystallographic direction, the magnitude of E_{cs} (meV/unit cell) is given by the length of the vector, the extremity of which lies on the 3D plot.

Moreover, it is worth emphasizing that the above atomic-scale study of interactions between CO₂ and CaO surfaces was inherently limited by the CO₂ configurations selected. More exhaustive exploratory approaches would help to confirm that no relevant configurations have been overlooked. To this aim, ab initio-based cluster expansions offer the most powerful tool, but their handling for CaO surfaces would probably be made difficult by the complexity of the crystallography, requiring to include the rotational degrees of freedom of the CO₃ groups. Moreover, such a task, untractable in presence of instabilities such as those detected on the (001) surface, would probably very instructive if applied to the (111) surface (possibly restricting to 2N configurations), as an efficient way to identify realistic arrangements of CO₂ acting as calcite precursors. Due to the large CO₂-induced atomic relaxations, reciprocal-space cluster expansions for complex structures²⁹ would be adequate, providing fruitful extensions of our analysis.

Finally, the strong sensitivity of CaCO₃ nucleation to the type of surface, as evidenced from our study, may have important practical consequences; as it provides a plausible explanation for the gradually decaying performances of the CaO-based devices employed for CO₂ storage. Indeed, the long-lasting cycles of CO₂ capture and release are probably accompanied by structural changes of the CaO matrix, notably surface evolution towards the most stable (001) surface, which appears to be unfavourable to calcite nucleation, as well as shrinking of the portion of “active” (111) surface.

CONCLUSIONS

The present work was devoted to an atomic-scale investigation, by means of density-functional method, of calcite nucleation in CaO surfaces. It reveals several features with practically important

consequences. Firstly, the (100) surface appears unfavourable for nucleation, due to strong structural instabilities related with CO₂ insertion. Conversely, the (111) surface emerges as a good candidate for CaCO₃ formation. We propose a layer-by-layer mechanism for this phenomenon, namely a lateral spreading of the CO₃ groups in the (111) surface leading to a thin nucleus with many CO₂ vacancies, followed by in-depth growth of the CaCO₃ layer. While our analysis also provides useful hints for understanding properties typical of calcite, such as off-stoichiometry and 30° rotation of the CO₃ groups, it points out these issues as challenges for future works. Moreover, through the “constituent strain energy” approach, the elastic properties of CaO//CaCO₃ coherent layers with various interface orientations are found a useful way to interpret the atomic-scale results, especially the special role of the (111) surface in nucleation. Finally, our study provides a hint to understand the practically important issue of lowered performances noted in CO₂ storage devices when the number of operating cycles increases.

REFERENCES

- [1] Bright, N.F.H.; Garner, W.E. Nucleus Formation on Crystals of Copper Sulphate Pentahydrate. *J. Chem. Soc.* 1934, 1872–1877.
- [2] Bertrand, G.; Comperat, M.; Lallemant, M.; Watelle, G. Variété et Evolution des Formes des Domaines Transformés sur Lames Monocristallines. *Ann. Chim.: Sci. Mat.* 1979, 4, 77–84.
- [3] Guarini, G.G.T.; Dei, L. Reorganization of Surface Layers of Crystal Hydrates in Dehydration/Rehydration Experiments. *J. Chem. Soc. Faraday Trans. 1* 1983, 79, 1599–1604.
- [4] Watelle, G.; Bertrand, G.; Lallemant, M. La Chimie Créatrice de Formes: Illustrations du Rôle de l’Ecart à l’Equilibre dans les Transformations de Systèmes Hétérogènes. *J. Chim. Phys.* 1987, 84, 1339–1351.
- [5] Tanaka, H.; Koga, N. Polarizing Microscopy for Examining Mechanisms of the Decomposition of Single Crystal Materials. *Thermochim. Acta* 1988, 133, 227–232.
- [6] Tanaka, H.; Koga, N.; Galwey, A.K. Thermal Dehydration of Crystalline Hydrates - Microscopic Studies and Introductory Experiments to the Kinetics of Solid-State Reactions. *J. Chem. Educ.* 1995, 72, 251–256.
- [7] Garner, W.E.; Pike, H.V. Dehydration Nuclei on Crystals of Copper Sulphate Pentahydrate. *J. Chem. Soc.* 1937, 1565–1568.
- [8] Bertrand, G.; Comperat, M.; Lallemant, M.; Watelle, G. Endothermic Decompositions of Inorganic Monocrystalline Thin Plates. I. Shape of Polycrystalline Product Domains Versus Constraints and Time. *J. Solid State Chem.* 1980, 32, 57–66.
- [9] Masuda, Y.; Iwata, K.; Ito, R.; Ito, Y. Kinetics of the Thermal Dehydration of Magnesium Oxalate Dihydrate in a Flowing Atmosphere of Dry Nitrogen. *J. Phys. Chem.* 1987, 91, 6543–6547.
- [10] Koga, N.; Tanaka, H. Kinetics and Mechanism of the Isothermal Dehydration of Zinc Acetate Dihydrate. *Thermochim. Acta* 1997, 303, 69–76.

- [11] Allen, J. P.; Parker, S. C.; Price, D. W. Atomistic Simulation of the Surface Carbonation of Calcium and Magnesium Oxide Surfaces. *J. Phys. Chem. C* 2009, 113, 8320-8328.
- [12] Allen, J. P.; Marmier, A.; Parker, S. C. Atomistic Simulation of the Surface Selectivity on Carbonate Formation at Calcium and Magnesium Oxide Surfaces. *J. Phys. Chem. C* 2012, 116, 13240-13251.
- [13] Li, Z.; Fang, F.; Tang, X; Cai, N. Effect of Temperature on the Carbonation Reaction of CaO with CO₂. *Energy and Fuels* 2012, 26, 2473-2482.
- [14] Li, Z.; Sun, H.; Cai, N. Rate Equation Theory for the Carbonation Reaction of CaO with CO₂. *Energy and Fuels* 2012, 26, 4607-4616.
- [15] Besson, R.; Rocha Vargas, M.; Favergeon, L. CO₂ Adsorption on Calcium Oxide: An Atomic-Scale Simulation Study. *Surface Science* 2012, 606, 490-195.
- [16] Favergeon, L.; Pijolat, M.; Valdivieso F.; Helbert C. Experimental Study and Monte-Carlo Simulation of the Nucleation and Growth Processes during the Dehydration of Li₂SO₄·H₂O Single Crystals. *Phys. Chem. Chem. Phys.* 2005, 7, 3723-3727.
- [17] Galwey, A.K.; Spinicci, R.; Guarini, G.G.T. Nucleation and Growth Processes Occurring during the Dehydration of Certain Aluns: the Generation, the Development and the Function of the Reaction Interface. *Proc. R. Soc. Lond. A* 1981, 378, 477-505.
- [18] Favergeon, L.; Pijolat, M.; Helbert, C. A Mechanism of Nucleation during Thermal Decomposition of Solids, *J. Mater. Sci.* 2008, 43, 4675-4683.
- [19] Hu, S. Y.; Baskes, M. I.; Stan, M.; Chen, L. Q. Atomistic Calculations of Interfacial Energies, Nucleus Shape and Size of θ' Precipitates in Al-Cu Alloys. *Acta Mater.* 2006, 54, 4699-4707.
- [20] Laks, D. B.; Ferreira, L. G.; Froyen, S.; Zunger, A. Efficient Cluster Expansion for Substitutional Systems. *Phys. Rev. B* 1992, 46, 12587-12605.
- [21] Thuinet, L.; Besson, R. New Insights on Strain Energies in Hexagonal Systems. *Appl. Phys. Lett.* 2012; 100, 251902(1-4).
- [22] Kresse, G.; Furthmüller, J. Efficient Iterative Schemes for Ab Initio Total-Energy Calculations Using a Plane-Wave Basis Set. *Phys. Rev. B* 1996, 54, 11169-11186.
- [23] Kresse, G.; Furthmüller, J. Efficiency of Ab Initio Total Energy Calculations for Metals and Semiconductors Using a Plane-Wave Basis Set. *Comput. Mater. Sci.* 1996, 6, 15-50.
- [24] Perdew, J. P.; Burke, K.; Ernzerhof, M. Generalized Gradient Approximation Made Simple. *Phys. Rev. Lett.* 1996, 77, 3865-3868.
- [25] Thuinet, L.; Besson, R. Ab Initio Study of Competitive Hydride Formation in Zirconium Alloys. *Intermetallics* 2012, 20, 24-32.
- [26] Wang, H; Li, M. Ab Initio Calculations of Second-, Third-, and Fourth-Order Elastic Constants for Single Crystals. *Phys. Rev. B* 2009, 79, 224102-224111.

[27] Kaga, H. Third-Order Elastic Constants of Calcite. *Phys. Rev.* 1968, 172, 900-919.

[28] Shanker, J.; Singh, J. P. Third- and Fourth-Order Elastic Constants for Silver Halides, Alkaline Earth Oxides, and Chalcogenides of Pb and Sn. *Phys. Stat. Sol. (a)* 1982, 70, 677-681.

[29] Holliger, L.; Besson, R. Reciprocal-Space Cluster Expansions for Complex Alloys with Long-Range Interactions. *Phys. Rev. B* 2011, 83, 174202(1-6).